A multigrid waveform relaxation method for solving the nonlinear silicon problem with relaxing boundary conditions

Priscila Dombrovski Zen, Marcio Augusto Villela Pinto & Sebastião Romero Franco

Published online: 10 May 2024.

Submit your article to this journal ↗

View related articles ↗

View Crossmark data ↗

Taylor & Francis
Taylor & Francis Group

Check for updates

A multigrid waveform relaxation method for solving the nonlinear silicon problem with relaxing boundary conditions

Priscila Dombrovski Zen[a] (iD), Marcio Augusto Villela Pinto[b] (iD), and Sebastião Romero Franco[c] (iD)

[a]Graduate Program in Numerical Methods in Engineering, Federal University of Paraná, Curitiba, Brazil; [b]Department of Mechanical Engineering, Federal University of Paraná, Curitiba, Brazil; [c]Department of Mathematics, State University of Centro-Oeste, Irati, Brazil

ABSTRACT

This paper introduces a multigrid FAS Waveform Relaxation method (FAS-MGWR) for solving a heat transfer model in a thin and homogeneous silicon bar with constant density and heat capacity. This method exhibits versatility, making it applicable to a range of problems including electronic device engineering, numerical simulation of nanofluids, among others. The Finite Difference Method with central differences (CDS) for spatial discretization and the Crank-Nicolson method for temporal approximation were utilized. Comparison with literature results and code verification demonstrated that irrespective of the combinations of physical and numerical parameters, the apparent order of discretization error converges to the theoretical asymptotic order. The study underscores the superior performance of the proposed FAS-MGWR method, notable for its parallel architecture, particularly in terms of computational time, compared to existing literature. Notably, the FAS-MGWR method was found to have excellent convergence factor and speed-up in relation to its singlegrid version, underscoring its efficiency and practical advantage in addressing complex thermal problems.

1. Introduction

Nonlinear heat equations play a central role in several areas of research, encompassing applications ranging from the thermal processing of materials and semiconductors to the study of heat transfer in porous media, laser thermotherapy and the analysis of heat transfer in a variety of contexts [1–7]. Within these areas, heat transfer by conduction performs is fundamental role, with applications including the modeling of temperature-dependent thermal conductivity, studies involving nanofluids and their application in the processing of semiconductor chips, as well as the analysis of heat transfer in human tissues and topological optimization, among others [8–10].

The solution of nonlinear heat equations has been approached through the development of several numerical techniques. For example, Filipov et al. [5] explored the dependence of thermal conductivity in semiconductors, using the Finite Difference Method and Newton's method for nonlinear systems; Zhuang et al. [8] used Newton's method to treat nonlinear heat conduction problems, involving topological optimization and complex constraints. Schaum et al. [7] observed the surface temperature of silicon wafers in production processes employing nonlinear heat equations in one dimension and cylindrical coordinates.

Nomenclature

a, b	Spatial ends of the silicon rod	v	Tank volume
c	Mean heat transfer coefficient	x	Spatial direction
c_p	Thermal capacity under constant pressure		
h	Spacing between discretized points	**Greek symbols**	
it	Number of iterations (in the singlegrid case) or cycles (in the multigrid case)	β	Constant in Dirichlet boundary condition
n	Time step n	ϕ_1	Solution in fine grid Ω^{h_1}
N	Total number of unknowns	ϕ_2	Solution in coarse grid Ω^{h_2}
N_t	Number of time steps in discretization	ϕ_3	Solution in super-coarse grid Ω^{h_3}
N_x	Number of points in spatial discretization	γ	Method coefficient
p	Complexity order	κ	Thermal conductivity of silicon
p_L	Asymptotic order discretization error	κ_0	Silicon density
p_U	Apparent order discretization error	ν_1	Number of pre-smoothing
q	Refinement ratio	ν_2	Number of post-smoothing
Q	Volume flow rate	ρ	Density of the silicon rod
r_0	Initial residue	ρ_m	Average convergence factor
r_{it}	Infinity norm of dimensionless residue at it-th iteration or cycle	τ	Time interval between time steps
		χ	Temperature distribution constant
S	Speed-up	ϵ	Stopping criterion
t	Time coordinate		
t_{CPU}	Computational time	**Acronyms**	
T	Temperature in the tank		
T_0	Initial temperature in the tank	FAS	Full Approximation Scheme
T_r	Liquid temperature in the tank	GSWR	Gauss-Seidel Waveform Relaxation
u	Temperature variable	MG	Multigrid method
u_c	Temperature at the central node	SG	Singlegrid method
u_m	Average temperature	WR	Waveform Relaxation

Among the numerical techniques widely used to solve systems of equations (among them, linear and nonlinear ones), the multigrid method stands out [11, 12]. This method is very useful in solving systems resulting from the discretization of differential equations that describe a variety of physical phenomena [13–16]. The multigrid method utilizes a hierarchy of grids and applies smoothing at these different levels to accelerate convergence. Studies have shown that this approach often results in faster convergence compared to conventional iterative methods that do not benefit from multigrid [17].

In the context of applying the multigrid method to nonlinear problems, [18] discusses two fundamental approaches. The first involves the use of a linearization scheme followed by the multigrid method to solve the linear system generated at each iteration. In this case, it is possible use, for example, Newton's method (referred to as Newton-MG). The second approach, described in Henson [18] and Brandt [19], discusses the Full Approximation Scheme (FAS), applying multigrid concepts directly in nonlinear contexts.

A comparison between the FAS and the Newton-MG approaches was carried out by Brabazon et al. [20]. In that work, the results are provided for elliptical and parabolic problems discretized with the Finite Element Method, demonstrating a shorter execution time, as well as greater stability of the Newton-MG iteration. Furthermore, the same authors demonstrate that the FAS iteration may be more advantageous than a Newton iteration in certain situations due to lower memory requirements. This characteristic makes the FAS iteration preferable in scenarios with large-scale problems, where memory available can be a limiting factor. Apart from its memory efficiency, the FAS method is distinguished by its flexibility in selecting algorithm components.

Luo et al. [21] conducted a comparison between the FAS and Newton-MG approaches in solving the system of poroelasticity equations for an incompressible fluid, considering hydraulic

conductivity dependent on stress and fluid pressure (characterizing a nonlinear problem). The numerical results demonstrated a good convergence performance for all strategies and also indicated that the FAS with Gauss-Seidel smoother with lexicographic ordering exhibited highly satisfactory convergence.

In addition to the above, we can think of different time sweeps, such as the Waveform Relaxation (WR) method [22]. This method has attracted considerable attention as an efficient iterative approach to solving large linear systems that arise from the discretization of transient differential equations. Its origins are traced back to researchers such as [22–24], who demonstrated the basic WR process and that it can be accelerated using multigrid concepts. Gaspar and Rodrigo [3] developed an efficient approach to the heat problem using the time-fractional WR method, obtaining robust and efficient results, while Franco et al. [4] proposed the MGWR method as a space-time solver for poroelasticity equations. Malacarne et al. [25] employed an approach combining WR with division into temporal subdomains to solve the 1D and 2D wave equations, achieving accurate results and notable improvements in convergence factors, acceleration, and reduction of initial oscillations. This approach resulted in a significant reduction in data processing time.

Several realistic nonlinear problems solved with different numerical techniques can be seen below. The problem of convective transport of pulsatile multilayer hybrid nanofluid flow and bioconvected tangent hyperbolic nanofluid flow, are studied in Jakeera et al. [26] and Ramasekhar et al. [27].

The study of entropy production as a means of quantifying energy dissipation in biological systems has garnered growing interest among biomedical engineers and clinicians. An analysis of the heat transfer behavior of the magnetohydrodynamic blood based Casson hybrid nanofluid in the occurrence of a non-Fourier heat flux model can be found in Shanmugapriyan and Jakeer [28].

Studies by Jakeer et al. [29] and Jakeer et al. [30] delve into a numerical simulation of biomagnetic nanofluid flow in the human circulatory system and a study of the influence of induced magnetic fields and double-diffusive convection on Carreau nanofluid flow through diverse geometries.

In this paper, we present the nonlinear heat transfer equation, which includes relaxing boundary conditions, in a setting involving a silicon rod. Recently, Filipov et al. [9] addressed relaxing boundary conditions together with convective and Dirichlet conditions using the Finite Difference Method (MDF), Euler's Method, and Newton's method for solving linear systems directly. Such boundary conditions were first introduced in diffusion processes and later applied to other heat transfer problems. In general terms, a relaxing boundary condition is a transient boundary condition that continually approaches the steady state. Such a condition can be of the Dirichlet, Neumann or Robin type [31].

Moreover, we propose to solve the nonlinear silicon rod problem with relaxing boundary conditions, as addressed by [9], in improve the convergence of the solution. To achieve this goal, we emphasize the use of the multigrid method, particularly focusing on the Full Approximation Scheme (FAS) approach, which has proven effective in addressing the nonlinearity of the problem. Additionally, we introduce the concept of Waveform Relaxation (WR), a method that favors parallel architecture and integrates seamlessly with the multigrid method and FAS, referred to here as FAS-MGWR.

The structure of this paper is organization as follows: In Section 2, we discuss the mathematical model and discretization of the nonlinear problem, along with its boundary conditions, using Finite Difference Methods and the Crank-Nicolson scheme. In Section 3, we present the Waveform Relaxation method associated with multigrid, with a focus on the FAS technique. In Section 4 includes code verification and showcases the main results of this work. Finally, Section 5 highlights the main conclusions.

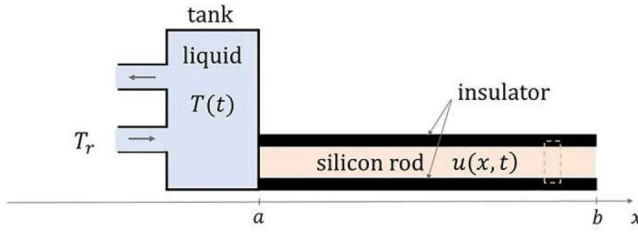## 2. Nonlinear heat equation and its discretization

Figure 1. Physical system.

In this section, we present a mathematical model of a physical problem involving heat convection in a silicon rod. This problem entails a nonlinear aspect due to the variation of thermal conductivity with temperature, and it is accompanied by relaxing boundary conditions.

Let us consider a silicon rod positioned along the x axis, with $x \in [a, b]$, as illustrated in Figure 1. The temperature of the rod over time represented by $u(x, t)$.

At the point $x = a$ in this Figure 1, the rod is in thermal contact with a tank filled with liquid. Heat can flow freely through the contact surface in both directions. In addition to thermal contact with the silicon, the tank is thermally insulated. The temperature within the tank, denoted by $T(t)$, is homogeneous, expect for a thin layer near the contact surface with the silicon. Two pipes are connected to the tank: one pumps liquid at temperature T_r into the tank at a constant flow rate, and the other allows the liquid at temperature $T(t)$ to leave the tank at the same flow rate. We assume that the liquid in the tank is stirred throughout the process, ensuring that the incoming liquid quickly mixed with the liquid inside the tank. Furthermore, we assume that the density and thermal capacity of the liquid do not vary with temperature [9], as depicted in Figure 1.

Therefore, the transient nonlinear partial differential equation that describes the convection of heat in this silicon rod, is given by [9]

$$\rho \ c_p \frac{\partial u}{\partial t} = \frac{\partial}{\partial x}\left(\kappa(u)\frac{\partial u}{\partial x}\right), x \in (a, b), t > 0, \tag{1}$$

where $u(x, t)$ represents the temperature at a position x and at an instant of time t, while ρ refers to the density of the silicon rod, and c_p represents the thermal capacity under constant pressure. The thermal conductivity of silicon is depicted by $\kappa(u) = \kappa_0 e^{\chi u}$, where κ_0 and χ denote, respectively, the physical parameters silicon density and temperature distribution constant [9, 31, 32]. This representation allows for the initial temperature distribution on the silicon rod at the moment $t = 0$ to be expressed as

$$u(x, 0) = u_0(x), x \in [a, b]. \tag{2}$$

We will consider that the temperature in the tank, in $t = 0$ is given by T_0. If the inlet liquid temperature T_r is different from T_0, the temperature in the tank $T(t)$ will change over time. This transfer of energy through the tubes is convective, meaning that liquid with a certain energy density replaces liquid with a different energy density. Therefore, the total energy in the tank is changing. Under this condition, the temperature at the boundary gradually increases or decreases with time, approaching a finite value. Thus, using the initial condition T_0, we obtain

$$T(t) = T_r + (T_0 - T_r)e^{-\frac{Q}{v}t}, \tag{3}$$

where Q and v represent, respectively, the flow rate of the inlet liquid volume and tank volume. It is worth noting that, under this condition, the temperature at this boundary gradually increases

with time, approaching a finite value. This approximation is given by a function that relaxes exponentially.

At the boundary condition at $x = a$, referred to as the convective boundary condition, the energy flow expressed through the thermal conductivity and temperature gradient in silicon is equated to the same energy flow given by the transport properties and the state of the liquid system. In other words,

$$-\kappa(u(a,t))\frac{\partial u(x,t)}{\partial x}\bigg|_{x=a} = c(T(t) - u(a,t)), t > 0, \tag{4}$$

where c denotes the average convective heat transfer coefficient. The condition given by Equation (4) is valid for solid-liquid contact surfaces, where the heat transport mechanism is mainly due to convection in the liquid system. For this type of boundary condition, the temperature on the surface $u(a,t)$ is considered essentially different from the temperature $T(t)$ inside the tank. As can be seen from Equation (3), as time increases, the function $T(t)$ approaches the constant value T_r. Therefore, the condition given by Equation (4) will be referred to as the convective relaxing boundary condition [9].

For the right boundary, $x = b$, we will consider the Dirichlet boundary condition

$$u(b,t) = \beta, t > 0, \tag{5}$$

where β is a constant.

When modeling important problems like this, which are analytically difficult or even impossible to solve, we resort to numerical methods for this task.

Using the chain rule on $\frac{\partial\kappa(u)}{\partial u}$, we obtain $\kappa_0\chi e^{\chi u} = \chi\kappa(u)$. Thus, we can rewrite Equation (1) as

$$\rho c_p \frac{\partial u}{\partial t} = \chi\kappa(u)\left(\frac{\partial u}{\partial x}\right)^2 + \kappa(u)\frac{\partial^2 u}{\partial x^2}. \tag{6}$$

We introduce a uniform spatial grid in

$$x \in [a,b] : x_i = a = (i-1)h, \tag{7}$$

with $i = 1, 2, 3, \cdots, N_x$ and $h = \frac{b-a}{N_x - 1}$ where N_x is the number of points in the discretization.

For temporal approximation, we have

$$t_n = n\tau, \tau = \frac{t_f - t_0}{N_t - 1}, n = 1, 2, 3, ..., N_t, \tag{8}$$

where t_0 and t_f represent the initial time and final time, respectively, and N_t is the total number of in time.

Using the Crank-Nicolson Method (CN) for temporal approximation and the Finite Difference Method (MDF) with second-order central approximations (CDS) for spatial discretization, we have

$$\rho c_p \left(\frac{u_i^{n+1} - u_i^n}{\tau}\right) = \frac{1}{2}\left[\chi\kappa(u_i^{n+1})\left(\frac{u_{i+1}^{n+1} - u_{i-1}^{n+1}}{2h}\right)^2 + \kappa(u_i^{n+1})\left(\frac{u_{i+1}^{n+1} - 2u_i^{n+1} - u_{i-1}^{n+1}}{h^2}\right)\right.$$
$$\left. +\chi\kappa(u_i^n)\left(\frac{u_{i+1}^n - u_{i-1}^n}{2h}\right)^2 + \kappa(u_i^n)\left(\frac{u_{i+1}^n - 2u_i^n - u_{i-1}^n}{h^2}\right)\right]. \tag{9}$$

Regrouping the terms, we can rewrite them as

$$\left(\frac{\rho c_p}{\tau} + \frac{\kappa(u_i^{n+1})}{h^2}\right)u_i^{n+1} = \frac{\chi}{8h^2}\kappa(u_i^{n+1})\left(u_{i+1}^{n+1} - u_{i-1}^{n+1}\right)^2 + \frac{1}{2h^2}\kappa(u_i^{n+1})\left(u_{i-1}^{n+1} + u_{i+1}^{n+1}\right)$$
$$+ \frac{\chi}{8h^2}\kappa(u_i^n)\left(u_{i+1}^n - u_{i-1}^n\right)^2 + \frac{1}{2h^2}\kappa(u_i^n)\left(u_{i-1}^n - 2u_i^n + u_{i+1}^n\right) + \frac{\rho c_p}{\tau}u_i^n. \tag{10}$$

Considering

$$a_w = \frac{1}{2h^2}, a_{w2} = \frac{\chi}{8h^2}, a_{pa} = \frac{\rho c_p}{\tau}, \tag{11}$$

in Equation (10), we have the following for inner points

$$\left[a_{pa} + 2a_w\kappa(u_i^{n+1})\right]u_i^{n+1} = a_{w2}\kappa(u_i^{n+1})\left(u_{i+1}^{n+1} - u_{i-1}^{n+1}\right)^2 + a_w\kappa(u_i^{n+1})\left(u_{i-1}^{n+1} + u_{i+1}^{n+1}\right)$$
$$+ a_{w2} \kappa(u_i^n)\left(u_{i+1}^n - u_{i-1}^n\right)^2 + a_w\kappa(u_i^n)\left(u_{i-1}^n - 2u_i^n + u_{i+1}^n\right) + a_{pa}u_i^n. \tag{12}$$

For the left boundary, in $x = a$, i.e. $i = 1$, and using CDS in Equation (4), we have the following expressions for the time steps $n + 1$ and n.

$$u_0^{n+1} = u_2^{n+1} + \frac{2hc\left(T(t) - u_1^{n+1}\right)}{\kappa(u_1^{n+1})}, \tag{13}$$

and

$$u_0^n = u_2^n + \frac{2hc\left(T(t - \tau) - u_1^n\right)}{\kappa(u_1^n)}. \tag{14}$$

Thus, at $i = 1$ in Equation (12), we have

$$\left[a_{pa} + 2a_w\kappa(u_1^{n+1})\right]u_1^{n+1} = a_{w2}\kappa(u_1^{n+1})\left(u_2^{n+1} - u_0^{n+1}\right)^2 + a_w\kappa(u_1^{n+1})\left(u_0^{n+1} + u_2^{n+1}\right)$$
$$+ a_{w2}\kappa(u_1^n)\left(u_2^n - u_0^n\right)^2 + a_w\kappa(u_1^n)\left(u_0^n - 2u_1^n + u_2^n\right) + a_{pa}u_1^n. \tag{15}$$

3. FAS-MGWR solver

Partial Differential Equations (PDEs) play an essential role in modeling physical phenomena, providing a powerful mathematical framework to describe the behavior of physical systems over time and space. However, due to the complexity of many real-world systems, obtaining analytical solutions for such PDEs is often impractical or even impossible. As a result, the numerical approach becomes a valuable and necessary tool for understanding these phenomena.

In this context, the discretization of PDEs is common in numerical modeling, leading to the emergence of large systems of equations that need to be solved to obtain an approximate solution. However, solving these systems using direct methods is often inadvisable due to the high computational cost associated with inverting the coefficient matrix [33]. To efficiently solve these discretized systems, iterative methods are often employed, such as the weighted Jacobi method and the Gauss-Seidel (GS) method [33, 34]. However, these iterative methods encounter efficiency challenges when dealing with highly refined grids. As the number of iterations increases, the method tends to lose their ability to reduce the entire spectrum of errors rapidly. They may quickly reduce high-frequency errors (oscillatory modes) but struggle to address low-frequency errors (smooth modes).

The multigrid method, extensively studied by [12], stands out as a highly effective strategy in the iterative solution of systems of equations derived from the discretization of differential equations in modeling physical phenomena. References [11, 12, 35, 36] attest to its notable superiority in terms of convergence speed when compared to conventional iterative methods that do not incorporate this approach, referred to here as singlegrid method.

The multigrid method is based on essential principles that include the use of a hierarchy of grids and smoothing techniques at each grid level, thereby addressing error across all frequencies. This is achieved by transferring information between grids using restriction operators (which transfer information from the finer to the immediately coarser grid) and prolongation operators (which transfer information from the coarser to the immediately finer grid). The number of smoothings performed in the restriction and prolongation process is called, respectively, pre-smoothing (ν_1) and post-smoothing (ν_2). The way the method goes through the grids is referred to as a cycle; for this work, we use the V-cycle $V(\nu_1, \nu_2)$ [36].

Two main approaches are adopted with the multigrid method to tackle this type of problem. The correction scheme (CS), which focuses on correction through the residue, is indicated for linear problems. On the other hand, the Full Approximation Scheme (FAS), which focuses on correction through the residual and system solution, is more appropriate for addressing nonlinear problems. This scheme applies the concepts of the multigrid method directly to the nonlinear problem, transferring information related to both the residue and the solutions to the coarser grids involved. This eliminates the need to perform global linearizations and demonstrating its ability to smooth out irregularities in the error. [3]

In the discretization of nonlinear transient equations, the Waveform Relaxation (WR) method [3, 4, 22] stands out for its effectiveness in the temporal approach to differential equations. The WR algorithm differs from traditional time sweep approaches, such as the Time-Stepping (TS) method [37, 38], by transforming a Partial Differential Equation (PDE) into a system of Ordinary Differential Equations (ODEs). This transformation results in functions over time, where at each spatial point, an ODE is resolved in all time steps [4]. This iterative approach has demonstrated success in solving complex systems, favoring parallel programming architecture.

Algorithm 1 describes in detail the implementation of the FAS-MGWR method for the $V(\nu_1, \nu_2)$ cycle. In this case, the algorithm utilizes the Gauss-Seidel smoother with red-black ordering, together with the Waveform Relaxation (WR) method (GSWR). For the stopping criterion, we adopted the infinity norm of the dimensionless residue at the *it-th* iteration relative to the initial estimate, denoted by $_{it}$ and r_0, respectively, given by

$$\frac{\|r_{it}\|_\infty}{\|r_0\|_\infty} < \varepsilon. \tag{16}$$

Algorithm 1: FAS-MGWR(l)

1   Input data, initial, and boundary conditions.
2   **while**   Stopping criterion is not reached **do**
3   **if** $l = L_{\max}$ **then**
4   Solve the system $A_l(v^l) = f^l$ on the coarse grid $\Omega^{2^{l-1}h}$.
5   Compute the correction on the coarse grid $w^l = v^l - \overline{v}^l$.
6   **else**
7   Smooth ν_1 times $A_l(v^l) = f^l$ on the grid $\Omega^{2^{l-1}h}$ using GSWR.
8   Compute and restrict the defect $\overline{r}^{l+1} = I_{2^{l-1}h}^{2^l h}\left[f^l - A_l(v^l)\right]$.
9   Restrict the solution: $\overline{v}^{l+1} = I_{2^{l-1}h}^{2^l h} v^l$.
10   Compute the right-hand side $f^{l+1} = \overline{r}^{l+1} + A_{l+1}\overline{v}^{l+1}$.
11   Solve at the next level: **FAS-MGWR($l + 1$)**.
12   Interpolate the correction: $w^l = I_{2^l h}^{2^{l-1}h} w^{l+1}$

13   Correct the solution: $v^l \leftarrow v^l + w^l$.
14   Smooth ν_2 times $A_l(v^l) = f^l$ on the grid $\Omega^{2^{l-1}h}$ using GSWR.
15   Compute the correction: $w^l = v^l - \overline{v}^l$.
16   **end if**
17 **end while**

4. Results and discussions

In this section, we address transient nonlinear heat transfer in a thin silicon rod in thermal contact with a liquid medium undergoing convection-base heating or cooling. Additionally, we present the results of the numerical implementation of this scenario. To evaluate the implemented code, we perform a code verification by comparing the results obtained with those presented in [9]. Specifically, we consider a setting involving a thin and homogeneous rod along the axis x, with $x \in [1, 3]$, excluding sources of heat or radiation.

The source code was developed using the Fortran language and compiled with Microsoft's Visual Studio 2022 development environment. It was executed on a system equipped with a Intel® Core™ $i7 - 10510U$ processor, featuring a central processing unit (CPU) operating at 1.80 GHz and 16 GB of RAM.

In the case of the singlegrid (single-mesh method), we use the Gauss-Seidel solver solver with red-black ordering to numerically solve the generated systems. In all simulations involving the multigrid, the $V(1)$ cycle was used.

4.1. Code verification

Firstly, a comparison was made a comparison between the numerical solutions obtained by [9] and the numerical solutions implemented with our singlegrid and multigrid methods.

The problem parameters were defined based on the characteristics of the experiment [9], and their specifications are as follows: density (ρ) and heat capacity (c_p) are unitary constants. The values of the other constants used were $c = 0.1$, $\kappa_0 = 0.1$, and $\chi = 0.5$. On the left boundary, in $x = 1$, we have a convective relaxing boundary condition, given by Equation (4) and to the right, in $x = 3$, we have a Dirichlet condition, with $\beta = 1$, i.e. $u(3, t) = 1$. The initial condition and the estimate of the inner points of the domain for $t > 0$, are unitary.

Figure 2 depicts the comparison between the solutions obtained using our code implemented with singlegrid (SG) and multigrid (MG) methods, alongside the solutions presented in the article by [9]. The comparison was made using a tolerance of $\varepsilon = 10^{-12}$ in Equation (16). From this comparison, we observe a close agreement between our numerical results and the reference solution of [9]. This confirms the accuracy of the code implementation.

In this work, we will calculate the discretization error orders of numerical approximations, namely the apparent order p_U and asymptotic order p_L. The p_U is an important metric to evaluate the order of convergence of numerical methods. It allows checking *a posteriori* whether the order of numerical solutions tends to the asymptotic order of discretization errors as the spacing h is reduced. In the context of our study, where we do not have an analytical solution to analyze the behavior of the discretization error, we use the apparent order, which contributes to the robustness of the technique. For this, nodal solutions are required on three different grids.

Considering ϕ_1, ϕ_2 and ϕ_3 the solutions in fine (Ω^{h1}), coarse (Ω^{h2}) and super-coarse grids (Ω^{h3}), related, respectively to the spacing h_1, h_2 and h_3, and $q = \frac{h_3}{h_2} = \frac{h_2}{h_1}$ the refinement ratio, we have [39]
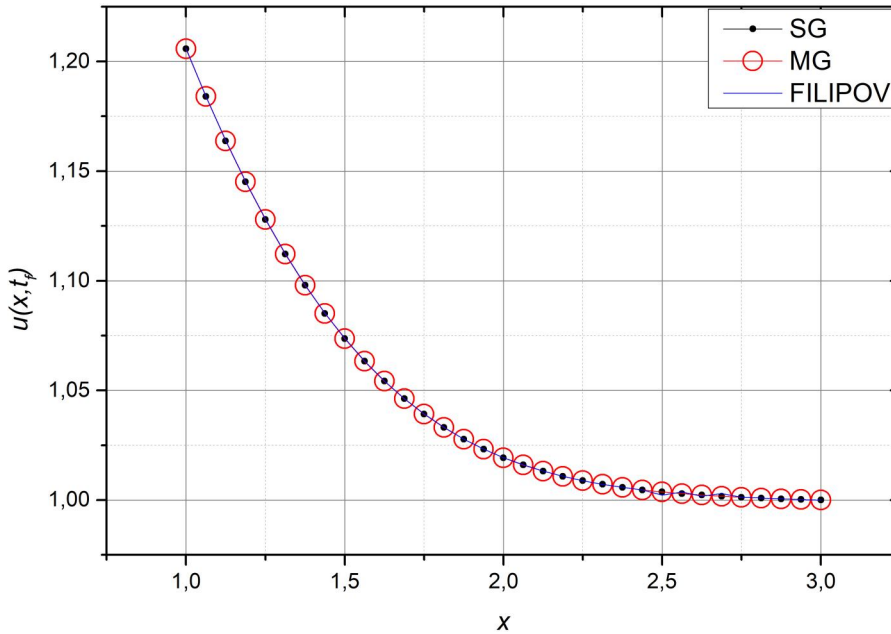
Figure 2. Comparison between Filipov/FASWR solutions.

$$p_U = \frac{\log\left|\frac{\phi_2 - \phi_3}{\phi_1 - \phi_2}\right|}{\log(q)}. \tag{17}$$

It is important to highlight that in our numerical simulations, we applied the Central Difference Scheme (CDS) method for spatial discretization and the Crank-Nicolson (CN) method for temporal discretization, both with an asymptotic order $p_L = 2$. Therefore, the asymptotic order of this numerical scheme must be $p_L = 2$.

In this work, the stopping criterion was adopted based on the drop in the dimensionless residual by the initial estimate. In this specific test, quadruple precision was used. Furthermore, the number of iterations performed was determined so that Equation (16) achieves the rounding error. This procedure was adopted to isolate the effects of discretization error, thus minimizing other sources of error.

In Figure 3, we consider the variables of interest to be the average temperature (u_m) and the temperature at the central point of the domain (u_c), both in the last time step and for some values of κ_0 and χ. Note that regardless of the specific combinations of κ_0 and χ, the apparent order (p_U) converges to 2 as the grid is refined. This pattern is consistent with our previous analysis, in which we used second-order methods for both the spatial and temporal discretizations of the problem.

It can be noted that in cases where $\kappa_0 = 10.0$, there is a greater oscillation of the apparent order p_U around the asymptotic order p_L for coarser grids, but it approaches the asymptotic order with grid refinement.

4.2. Numerical results

In this section, we will present the numerical results, for settings with combinations of $\kappa_0 = 0.1$ and 10.0, with $\chi = 0.5$ and 2.0 and using $\varepsilon = 10^{-12}$ as a stopping criterion in Equation (16). We will also use the parameters presented in the previous section.
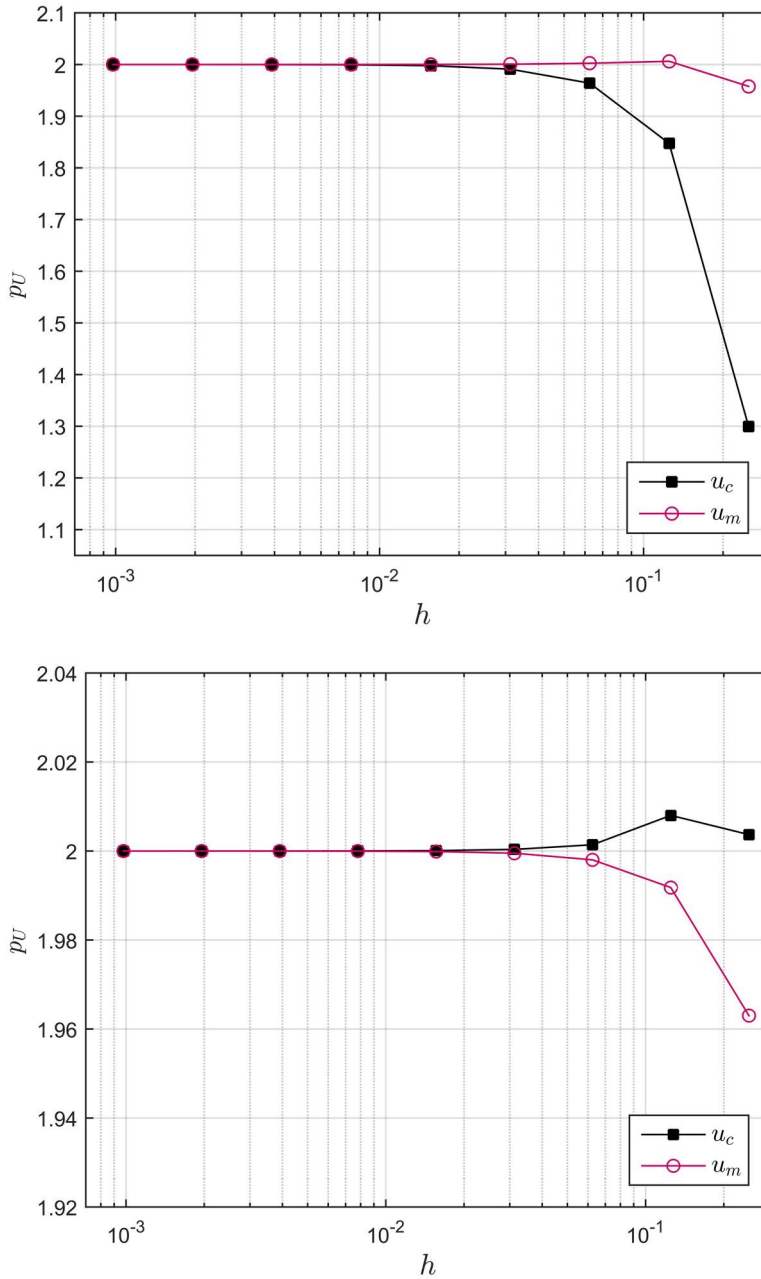
Figure 3. Apparent order.

4.2.1. Average convergence factor

In this results section, we will first analyze the average convergence factor (ρ_m) of the singlegrid and multigrid methods. To do this, we calculate the asymptotic convergence factor (ρ) through the following expression [12]

$$\rho(it) = \frac{\|res_{it}\|_\infty}{\|res_{it-1}\|_\infty},\tag{18}$$
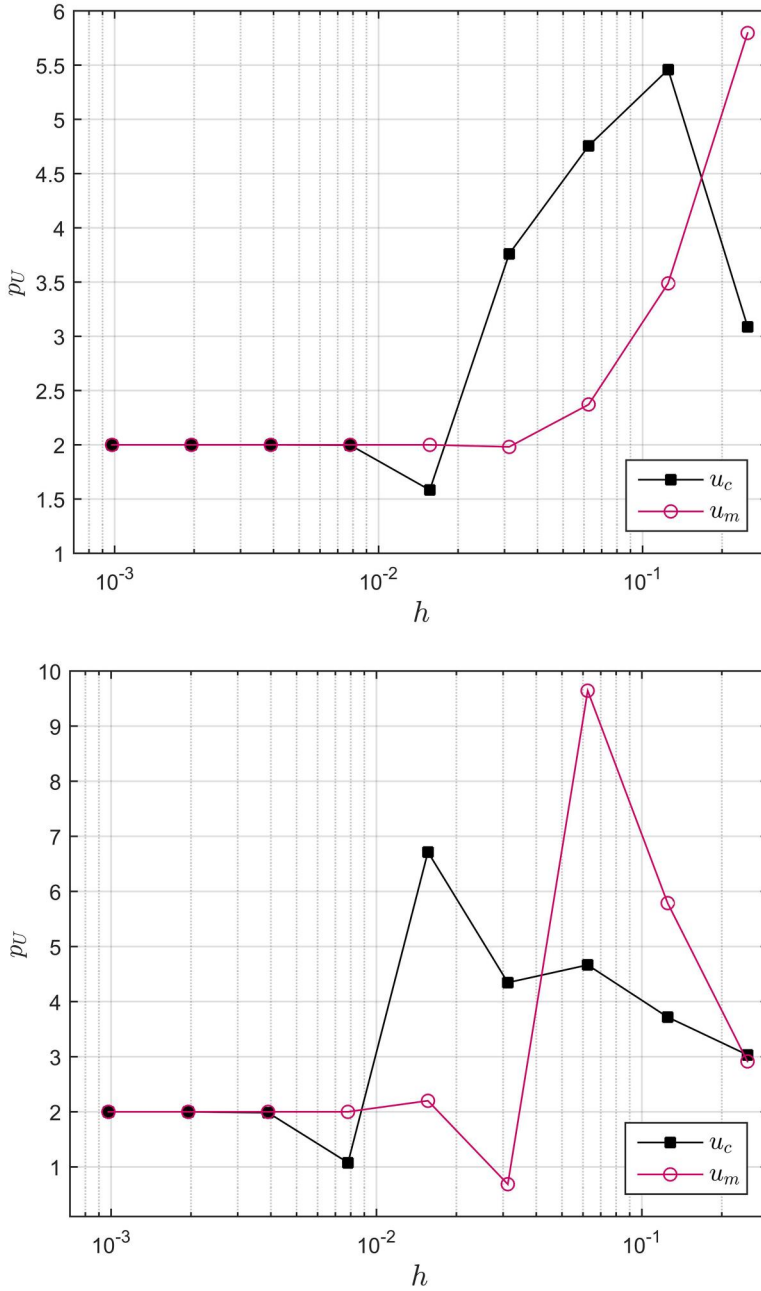
Figure 3. Continued.

where the value of *it* represents the number of iterations (in the singlegrid case) or cycles (in the multigrid case) performed.

Secondly, we analyze the average convergence factor given by [12]

$$\rho_m = \sqrt[it]{\rho(1).\rho(2).\cdots.\rho(it)}. \tag{19}$$

Figure 4 displays the average convergence factor (ρ_m) *versus* total number of unknowns $\mathbf{N} = (N_x - 1) \times (N_t - 1)$ (spatial and temporal unknowns).
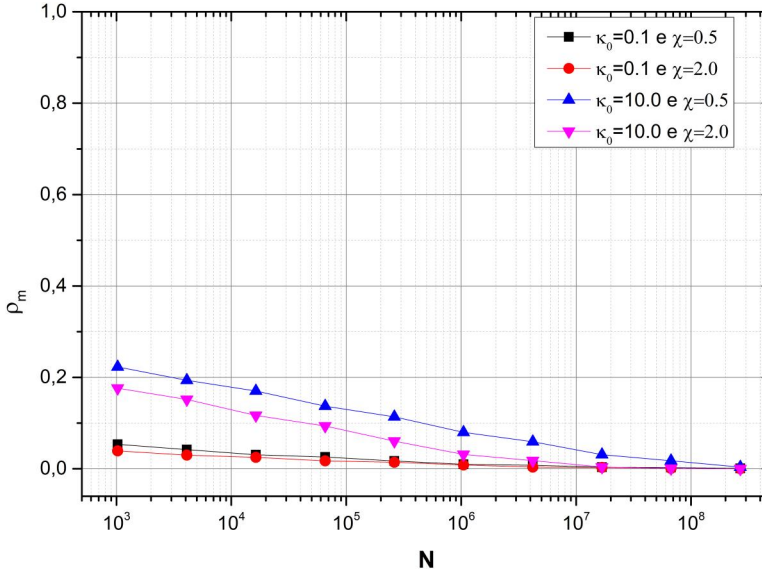
Figure 4. Average convergence factor. ρ_m

As the grid is refined, we observe that ρ_m tends to value close to zero, regardless of the physical parameters adopted. As we know, ρ_m close to zero indicates more efficient methods, while ρ_m close to unity indicates the opposite [11]. Therefore, Figure 4 indicates robustness and efficiency of the multigrid method.

4.3. CPU time, complexity, and speed-up

Now we will evaluate the performance of the singlegrid and multigrid methods using the concepts of complexity and speed-up. Evaluating the performance of such methods often considers computational time as a fundamental metric.

Figure 5 provides, on a two-logarithmic scale, a representation of computational time (t_{CPU}) in relation to $\mathbf{N}$, for the singlegrid method ($t_{CPU}(SG)$), multigrid ($t_{CPU}(MG)$), and the parameters adopted κ_0 and χ.

Notably, the multigrid method demonstrates a significant advantage compared to the singlegrid method in the t_{CPU} simulation run. For example, in the case with $\kappa_0 = 0.1$ and $\chi = 0.5$ (also present in [9]), for $N_x = N_t = 2049$ nodes, making up $\mathbf{N} = 4194304$ unknowns, the multigrid method took approximately 4.4s to reach the stopping criterion, while the singlegrid method required around 8200s.

To evaluate the order of complexity of the algorithms, which is a measure that indicates the amount of computational resources needed to solve the problem, we analyze the slope of the computational time lines (t_{CPU}) in relation to the number of unknowns, as already illustrated in Figure 5. Notably, the multigrid method demonstrates a significant advantage compared to the singlegrid method in the slope of its straight lines.

To evaluating such complexity, denoted as p, we applied a nonlinear adjustment [34, 40, 41], given by

$$t_{CPU}(\mathbf{N}) = \gamma \mathbf{N}^p, \tag{20}$$

where γ represents the method coefficient, p corresponds to the order of complexity and $\mathbf{N}$ is the total number of unknowns in the problem.

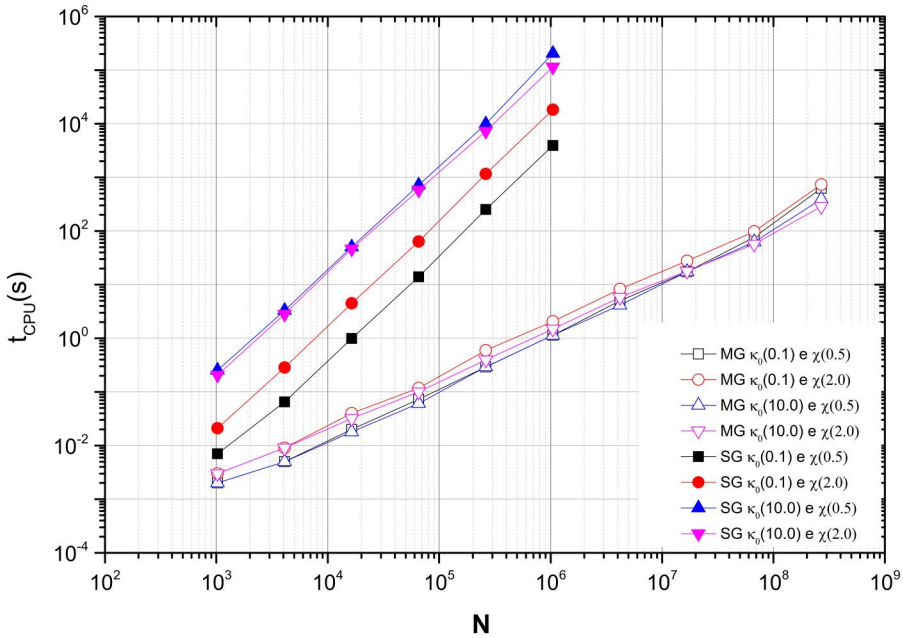**Figure 5.** Computational time.

Table 1. Order of complexity.

κ_0	χ	singlegrid		multigrid	
		γ	p	γ	p
0.1	0.5	1.897E-9	2.0408	7.071E − 7	1.0297
0.1	2.0	1.372E − 8	2.0256	1.358E − 6	0.9798
10.0	0.5	8.861E − 8	2.0619	2.752E − 6	0.9729
10.0	2.0	1.272E − 7	2.0046	1.820E − 6	0.9632

According to reference studies [11, 12, 35], the multigrid method is considered ideal when the order of complexity p approaches unity and γ tends to zero.

Table 1 presents the values of γ and p for the SG and MG methods for the physical parameters presented. As can be seen, these results agree with the literature.

Finally, we evaluate the Speed-up (S), a metric was adopted to measure the increase in speed of the multigrid algorithm in relation to the singlegrid, given by

$$S = \frac{t_{CPU}(SG)}{t_{CPU}(MG)}. \tag{21}$$

Note that in Figure 5, for example, for $\kappa_0 = 0.1$ and $\chi = 0.5$ (values used in [9]), with $\mathbf{N} = 2048 \times 2048$, we have $t_{CPU}(SG) \approx 8200s$, $t_{CPU}(MG) \approx 4.4s$ and $S \approx 1860$. This means that the multigrid method is approximately 1860 times faster than singlegrid method, which is evident in Figure 6, where we have S *versus* $\mathbf{N}$ for some parameter values $\kappa_0 = 0.1$ and $\chi = 0.5$. We can notice the significant advantage of the multigrid method for even larger values of $\mathbf{N}$, for example, $S \approx 200000$ for $\kappa_0 = 0.1$ and $\chi = 0.5$ in Figure 6.

Furthermore, the increasing behavior of the curves is notable, indicating an increase in S with the increase of $\mathbf{N}$, which is a highly desirable property.

Remark: As demonstrated in this section, numerical experiments were conducted to analyze the nonlinear heat equation with convective relaxation boundary condition. These experiments
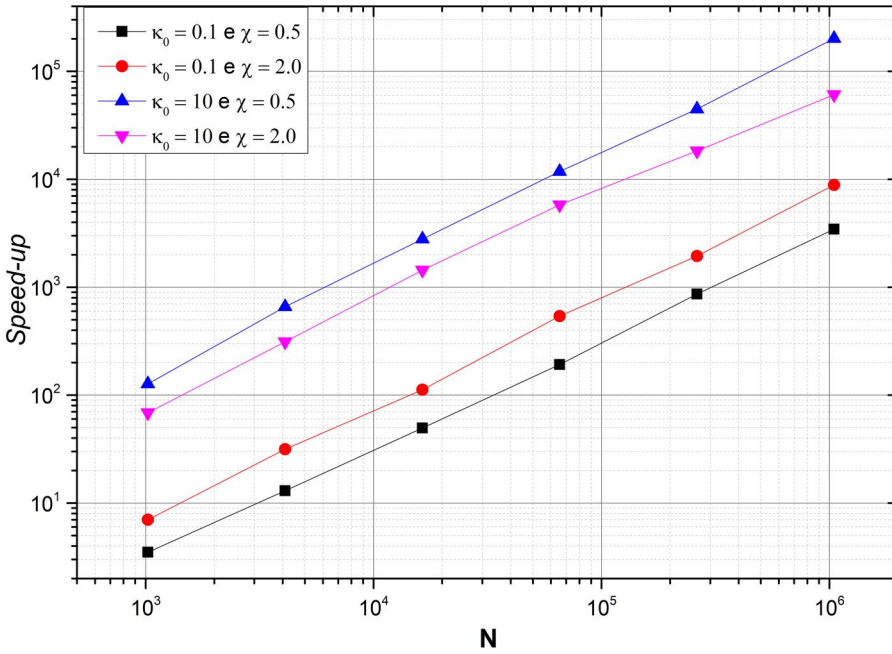
Figure 6. Speed-up.

investigated various physical parameters, including silicon density (κ_0), temperature distribution constant (χ), specific thermal capacity (c_p), material density (ρ), among others. The obtained results have broad applications, particularly in electronic device engineering, facilitating enhanced comprehension and control of nonlinear heat transfer phenomena. The methods developed in this study provide effective solutions to such challenges.

5. Conclusion

In this study, we introduced the Full Approximation Scheme multigrid method with temporal sweeping Waveform Relaxation (FAS-MGWR) for tackling nonlinear problems. Specifically, we addressed a one-dimensional nonlinear heat equation, modeling heat conduction in a silicon rod with relaxing boundary conditions. Our numerical approach involved employing the Crank-Nicolson method for temporal approximation and the Finite Difference Method (FDM) with a Central Difference Scheme (CDS) for spatial discretization. Through code verification and comparison with existing literature, we validated our methodology. The results, including the average convergence factor ρ_m, order of complexity p and Speed-up (S) underscored the efficiency and reliability of the FAS-MGWR method across various scenarios. These findings not only contribute to the advancement of numerical methods for tackling intricate thermal problems but also hold practical significance across industries, notably in the semiconductor sector.

Acknowledgments

Disclosure statement

Funding

ORCID

Priscila Dombrovski Zen (iD) http://orcid.org/0000-0001-7826-4928
Marcio Augusto Villela Pinto (iD) http://orcid.org/0000-0003-4166-4674
Sebastião Romero Franco (iD) http://orcid.org/0000-0002-4580-5924

References

[1]   F. P. Incropera, D. P. De Witt, T. Bergman and A. Lavine, *Fundamentals of Heat and Mass Transfer*. 6th ed. NJ, USA: John Wiley & Sons, 2006.
[2]   M. Becker, "Nonlinear transient heat conduction using similarity groups," *Int. J Heat Mass Transfer*, vol. 122, no. 1, pp. 33–39, 2000. DOI: 10.1115/1.521434.
[3]   F. J. Gaspar and C. Rodrigo, "Multigrid waveform relaxation for the time-fractional heat equation," *SIAM J. Sci. Comput.*, vol. 39, no. 4, pp. A1201–A1224, 2017. DOI: 10.1137/16M1090193.
[4]   S. R. Franco, C. Rodrigo, F. J. Gaspar, and M. A. V. Pinto, "A multigrid waveform relaxation method for solving the poroelasticity equations," *Comp. Appl. Math*, vol. 37, no. 4, pp. 4805–4820, 2018. DOI: 10.1007/s40314-018-0603-9.
[5]   S. M. Filipov and I. Faragó, "Implicit Euler time discretization and FDM with Newton method in nonlinear heat transfer modeling," *Int. Sci. J. Math. Model*, vol. 2, no. 3, pp. 94–98, 2018. DOI: 10.48550/arXiv.1811.06337.
[6]   X. Wang, T. Zeng, G. Xu, K. Zhang, and S. Yu, "Predicting the equivalent thermal conductivity of pyramidal lattice core sandwich structures based on Monte Carlo model," *Int. J. Therm. Sci.*, vol. 161, pp. 106701, 2021. DOI: 10.1016/j.ijthermalsci.2020.106701.
[7]   A. Schaum, *et al.*, "Observer design for a nonlinear heat equation: application to semiconductor wafer processing," *J. Process Control*, vol. 119, pp. 34–43, 2022. DOI: 10.1016/j.jprocont.2022.09.004.
[8]   C. Zhuang, Z. Xiong, and H. Ding, "Temperature-constrained topology optimization of nonlinear heat conduction problems," *J. Comput. Des. Eng*, vol. 8, no. 4, pp. 1059–1081, 2021. DOI: 10.1093/jcde/qwab032.
[9]   S. M. Filipov, I. Faragó, and A. Avdzhieva, "Mathematical modelling of nonlinear heat conduction with relaxing boundary conditions," *Int. Conf. Numer. Methods Appl*, vol. 13858, pp. 146–158, 2022. DOI: 10.1007/978-3-031-32412-3_13.
[10] C. D. Santiago, G. R. Ströher, M. A. V. Pinto and S. R. Franco, "A multigrid waveform relaxation method for solving the Pennes bioheat equation," *Numer. Heat Transf. Part A*, vol. 83, no. 9, pp. 976–990, 2023. DOI: 10.1080/10407782.2022.2156411.
[11] W. L. Briggs, V. E. Henson, and S. F. Mccormick, *A Multigrid Tutorial*, 2nd ed. Philadelphia, PA: SIAM, 2000.
[12] U. Trottenberg, C. W. Oosterlee, and A. Schuller, *Multigrid*. London, UK: Academic Press, 2001.
[13] R. Suero, M. A. V. Pinto, C. H. Marchi, L. K. Araki, and A. C. Alves, "Analysis of algebraic multigrid parameters for two-dimensional steady-state heat diffusion equations," *Appl. Math. Model*, vol. 36, no. 7, pp. 2996–3006, 2012. DOI: 10.1016/j.apm.2011.09.088.
[14] C. H. Marchi, *et al.*, "Repeated Richardson extrapolation applied to the two-dimensional Laplace equation using triangular and square grids," *Appl. Math. Model*, vol. 37, no. 7, pp. 4661–4675, 2013a. DOI: 10.1016/j.apm.2012.09.071.
[15] M. A. V. Pinto, C. Rodrigo, F. J. Gaspar, and C. W. Oosterlee, "On the robustness of ILU smoothers on triangular grids," *Appl. Math. Model*, vol. 106, pp. 37–52, 2016. DOI: 10.1016/j.apnum.2016.02.007.
[16] S. R. Franco and M. A. V. Pinto, "A space-time multigrid method for poroelasticity equations with random hydraulic conductivity," *Numer. Heat Transf. Part B*, vol. 106, pp. 1–10, 2023. DOI: 10.1080/10407790.2023.2262746.
[17] M. F. Malacarne, M. A. V. Pinto, and S. R. Franco, "Performance of the multigrid method with time-stepping to solve 1D and 2D wave equations," *Int. J. Comput. Methods. Eng. Sci. Mech., Taylor Francis*, vol. 23, no. 1, pp. 45–56, 2022. DOI: 10.1080/15502287.2021.1910750.

[18]   V. E. Henson, "Multigrid methods nonlinear problems: an overview," *Comp. Imaging*, vol. 5016, pp. 36–48, 2003. DOI: 10.1117/12.499473.

[19]   A. Brandt, "Multi-level adaptive solutions to boundary-value problems," *Math. Comp*, vol. 31, no. 138, pp. 333–390, 1977. DOI: 10.2307/2006422.

[20]   K. J. Brabazon, M. E. Hubbard, and P. K. Jimack, "Nonlinear multigrid methods for second order differential operators with nonlinear diffusion coefficient," *Comput. Math. Appl.*, vol. 68, no. 12, pp. 1619–1634, 2014. DOI: 10.1016/j.camwa.2014.11.002.

[21]   P. Luo, C. Rodrigo, F. J. Gaspar, and C. W. Oosterlee, "Multigrid method for nonlinear poroelasticity equations," *Comput. Visual Sci*, vol. 17, no. 5, pp. 255–265, 2015. DOI: 10.1007/s00791-016-0260-8.

[22]   S. Vandewalle and R. Piessens, "Numerical experiments with nonlinear multigrid waveform relaxation on a parallel processor," *Appl. Numer. Math., Elsevier*, vol. 8, no. 2, pp. 149–161, 1991. DOI: 10.1016/0168-9274(91)90048-5.

[23]   E. Lelarasmee, A. E. Ruehli, and S. A. L. Vincentelli, "The waveform relaxation method for time-domain analysis of large-scale integrated circuits," *IEEE Trans. Comput.-Aided Des. Integr. Circuits Syst.*, vol. 1, no. 3, pp. 131–145, 1982. DOI: 10.1109/TCAD.1982.1270004.

[24]   C. Lubich and A. Ostermann, "Multigrid dynamic iteration for parabolic equations," *BIT Numer. Math*, vol. 27, no. 2, pp. 216–234, 1987. DOI: 10.1007/BF01934186.

[25]   M. F. Malacarne, M. A. V. Pinto, and S. R. Franco, "Subdomain method in time with waveform relaxation in space applied to the wave equation combined with the multigrid method," *Rev. Int. Mét. Numér. Cálculo. Diseño. Ing*, vol. 38, no. 4, pp. 39, 2022. DOI: 10.23967/j.rimni.2022.11.001.

[26]   S. Jakeer, R. R. Reddy, M. Rupa, and H. Basha, "Convective transport of pulsatile multilayer hybrid nanofluid flow in a composite porous channel," *NAMC*, vol. 29, no. 2, pp. 330–348, 2024. DOI: 10.15388/namc.2024.29.34489.

[27]   G. Ramasekhar, *et al.*, "Heat transfer exploration for bioconvected tangent hyperbolic nanofluid flow with activation energy and joule heating induced by Riga plate," *Case Stud. Therm. Eng.*, vol. 55, pp. 104100, 2024. DOI: 10.1016/j.csite.2024.104100.

[28]   N. Shanmugapriyan and S. Jakeer, "Biomedical aspects of entropy generation on MHD flow of TiO2-Ag/blood hybrid nanofluid in a porous cylinder," *Comput. Methods Biomech. Biomed. Eng.*, pp. 1–18, 2023. DOI: 10.1080/10255842.2023.2245520.

[29]   S. Jakeer, N. Shanmugapriyan, and S. R. R. Reddy, "Numerical simulation of bio-magnetic nanofluid flow in the human circulatory system," *Numer. Heat Transf. Part A. Appl.*, pp. 1–29, 2024. DOI: 10.1080/10407782.2024.2304046.

[30]   S. Jakeer, S. R. R. Reddy, S. V. Easwaramoorthy, H. T. Basha, and J. Cho, "Exploring the influence of induced magnetic fields and double-diffusive convection on carreau nanofluid flow through diverse geometries: a comparative study using numerical and ANN approaches," *Math*, vol. 11, no. 17, pp. 3687, 2023. DOI: 10.3390/math11173687.

[31]   Hriston, J., "On a non-linear diffusion model of wood impregnation: analysis, approximate solutions, and experiments with relaxing boundary conditions," *Adv. Math. Mod., Appl. Anal. Comp.*, pp. 25–53, 2022. DOI: 10.1007/978-981-19-0179-9_2.

[32]   J. A. Gbadeyan, E. O. Titiloye, and A. T. Adeosun, "Effect of variable thermal conductivity and viscosity on Casson nanofluid flow with convective heating and velocity slip," *Heliyon, Elsevier*, vol. 6, no. 1, pp. e03076, 2020. DOI: 10.1016/j.heliyon.2019.e03076.

[33]   G. H. Golub and J. M. Ortega, *Scientific Computing and Differential Equations: An Introduction to Numerical Methods*, New York: Academic Press, 1992.

[34]   R. L. Burden, J. D. Faires, and A. M. Burden, *Numerical Analysis*, 10th ed. Cengage Learning, 2016.

[35]   P. Wesseling, *An Introduction to Multigrid Methods*, Chichester: Wiley, 1992.

[36]   W. Hackbusch, *Multi-Grid Methods and Applications*, Berlin: Springer Science & Business Media, vol. 4, 2013.

[37]   J. C. Strikwerda, *Finite Difference Schemes and Partial Differential Equations*, SIAM: Philadelphia, 2004.

[38]   R. Wienands and W. Joppich, *Practical Fourier Analysis for Multigrid Methods*, Washington, USA: Chapman Hall/CRC Press, vol. 4, 2005.

[39]   L. P. da Silva, B. B. Rutyna, A. R. S. Righi, and M. A. V. Pinto, "High order of accuracy for Poisson equation obtained by grouping of repeated Richardson extrapolation with fourth order schemes," *Comput. Model. Eng. Sci.*, vol. 128, no. 2, pp. 699–715, 2021. DOI: 10.32604/cmes.2021.014239.

[40]   F. Oliveira, S. R. Franco, and M. A. V. Pinto, "The effect of multigrid parameters in a 3D heat diffusion equation," *Int. J. Appl. Mech. Eng.*, vol. 23, no. 1, pp. 213–221, 2018. DOI: 10.1515/ijame-2018-0012.

[41]   M. L. Oliveira, M. A. V. Pinto, S. F. T. Gonçalves, and G. V. Rutz, "On the robustness of the xy-zebra-Gauss-Seidel smoother on an anisotropic diffusion problem," *Comput. Model. Eng. Sci.*, vol. 117, no. 2, pp. 251–270, 2018. DOI: 10.31614/cmes.2018.04237.